Determination of diffractive parton densities at the LHeC and FCC-eh

Anna Staśto

PennState
Eberly College of Science

In collaboration with Nestor Armesto, Paul Newman and Wojciech Slominski

arXiv:1901.09076

XXVII Workshop on Deep Inelastic Scattering and Related Subjects, DIS2019, Torino, Italia, April 8-12, 2019

Outline

- Introduction: diffraction at HERA
- Phase space for inclusive diffraction at LHeC and FCC-eh
- Reduced cross section - pseudodata simulation
- Simulation of diffractive parton distribution functions
- Diffraction on nuclei

Introduction

What is diffraction ?

- Diffractive processes are characterized by the rapidity gap: absence of any activity in part of the detector.
- Diffraction is interpreted as to be mediated by the exchange of an ‘object’ with vacuum quantum numbers - usually referred to as the *Pomeron*.

At HERA in electron-proton collisions:
about 10% events diffractive

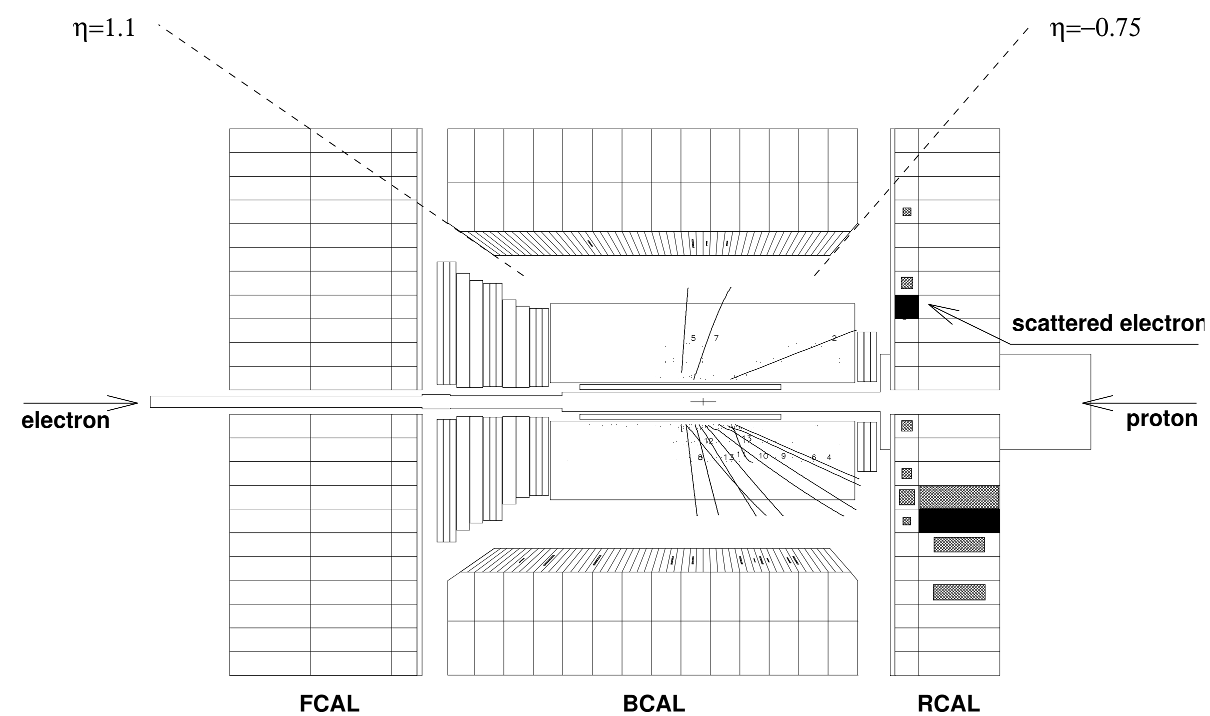

Diffractive event in ZEUS at HERA

Diffractive kinematics in DIS

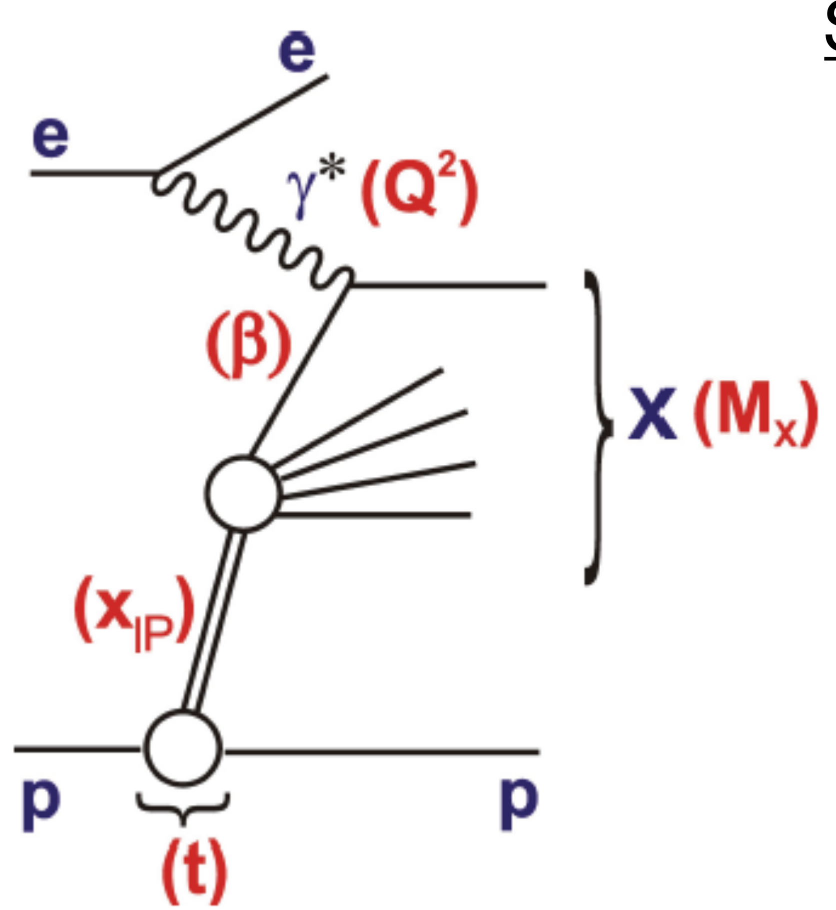

$$x_{Bj} = x_{IP}\beta$$

Standard DIS variables:

electron-proton
cms energy squared:

$$s = (k+p)^2$$

photon-proton
cms energy squared:

$$W^2 = (q+p)^2$$

inelasticity

$$y = \frac{p \cdot q}{p \cdot k}$$

Bjorken x

$$x = \frac{-q^2}{2p \cdot q}$$

(minus) photon virtuality

$$Q^2 = -q^2$$

Diffractive DIS variables:

$$\xi \equiv x_{IP} = \frac{Q^2 + M_X^2 - t}{Q^2 + W^2}$$

momentum fraction of
the Pomeron w.r.t hadron

$$\beta = \frac{Q^2}{Q^2 + M_X^2 - t}$$

momentum fraction of
parton w.r.t Pomeron

$$t = (p - p')^2$$

4-momentum transfer squared

Two classes of diffractive events in DIS:

$Q^2 \sim 0$ photoproduction

$Q^2 \gg 0$ deep inelastic scattering

Diffractive structure functions

$$\frac{d^3\sigma^D}{dx_{IP}\,dx\,dQ^2} = \frac{2\pi\alpha_{\rm em}^2}{xQ^4}\,Y_+\,\sigma_r^{D(3)}(x_{IP},x,Q^2)$$

$$Y_+ = 1 + (1-y)^2$$

Reduced diffractive cross section depends on two structure functions

$$\sigma_r^{D(3)} = F_2^{D(3)} - \frac{y^2}{Y_+}F_L^{D(3)}$$

For y not to close to unity we have: $\sigma_r^{D(3)} \simeq F_2^{D(3)}$

Integrated vs unintegrated structure functions over t:

$$F_{T,L}^{D(3)}(x,Q^2,x_{IP}) = \int_{-\infty}^{0} dt F_{T,L}^{D(4)}(x,Q^2,x_{IP},t)$$

$$F_2^{D(4)} = F_T^{D(4)} + F_L^{D(4)}$$

Collinear factorization in diffraction

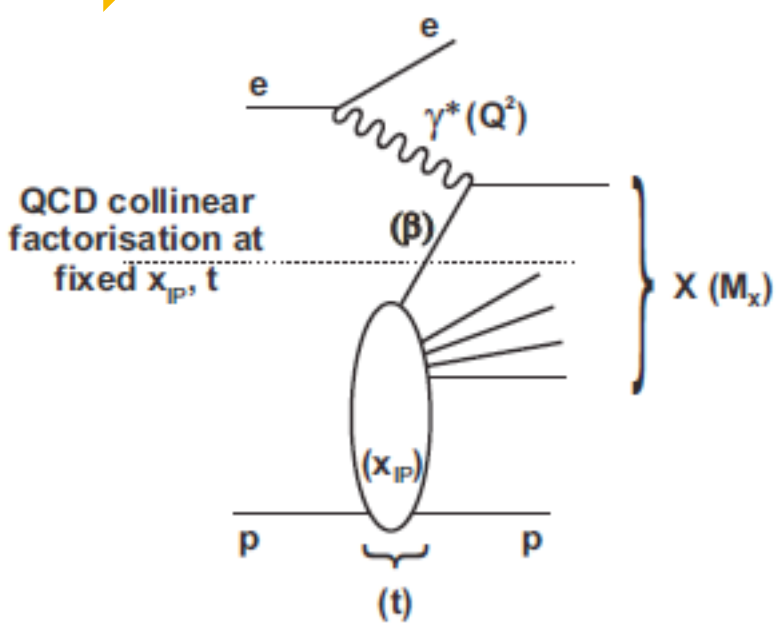

Collins

Collinear factorization in diffractive DIS

$$d\sigma^{ep\to eXY}(x,Q^2,x_{IP},t) \;=\; \sum_i f_i^D \otimes d\hat{\sigma}^{ei} \;+\; \mathcal{O}(\Lambda^2/Q^2)$$

- Diffractive cross section can be factorized into the convolution of the perturbatively calculable partonic cross sections and diffractive parton distributions (DPDFs).
- Partonic cross sections are the same as for the inclusive DIS.
- The DPDFs represent the probability distributions for partons *i* in the proton under the constraint that the proton is scattered into the system Y with a specified 4-momentum.
- Factorization should be valid for sufficiently(?) large Q^2 (and fixed t and x_{IP}).

DPDF parametrization

Regge factorization (additional assumption)

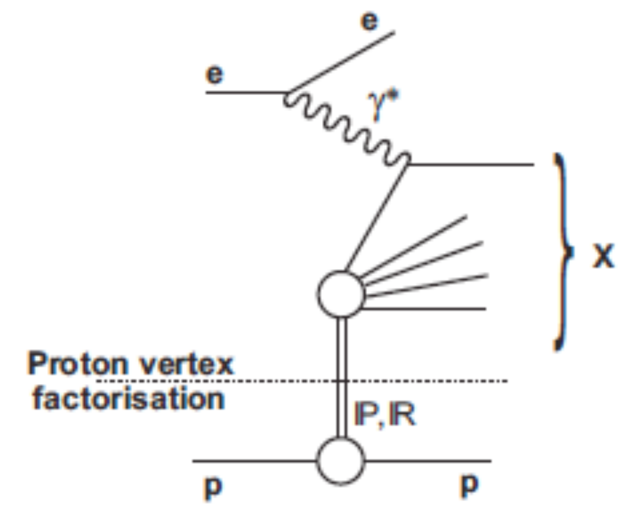

$$f_i^D(x,Q^2,x_{IP},t) = f_{IP/p}(x_{IP},t)\, f_i(\beta = x/x_{IP},Q^2)$$

Pomeron flux is parametrized as

$$f_{IP/p}(x_{IP},t) = A_{IP}\frac{e^{B_{IP}t}}{x^{2\alpha_{IP}(t)-1}}$$

$$\alpha_{IP}(t) = \alpha_{IP}(0) + \alpha'_{IP}t$$

parton distributions in the Pomeron

$$f_k(z) = A_k z^{B_k}(1-z)^{C_k}$$

where k=g,d. Light quarks equal u=d=s.

For good description of the data usually subleading Reggeons are included

$$f_i^D(x,Q^2,x_{IP},t) = f_{IP/p}(x_{IP},t)\, f_i(\beta,Q^2) + n_{IR} f_{IR/p}(x_{IP},t)\, f_i^{IR}(\beta,Q^2)$$

Diffractive fits

$\xi = x_{IP}$

Example of the DGLAP fit to the diffractive data

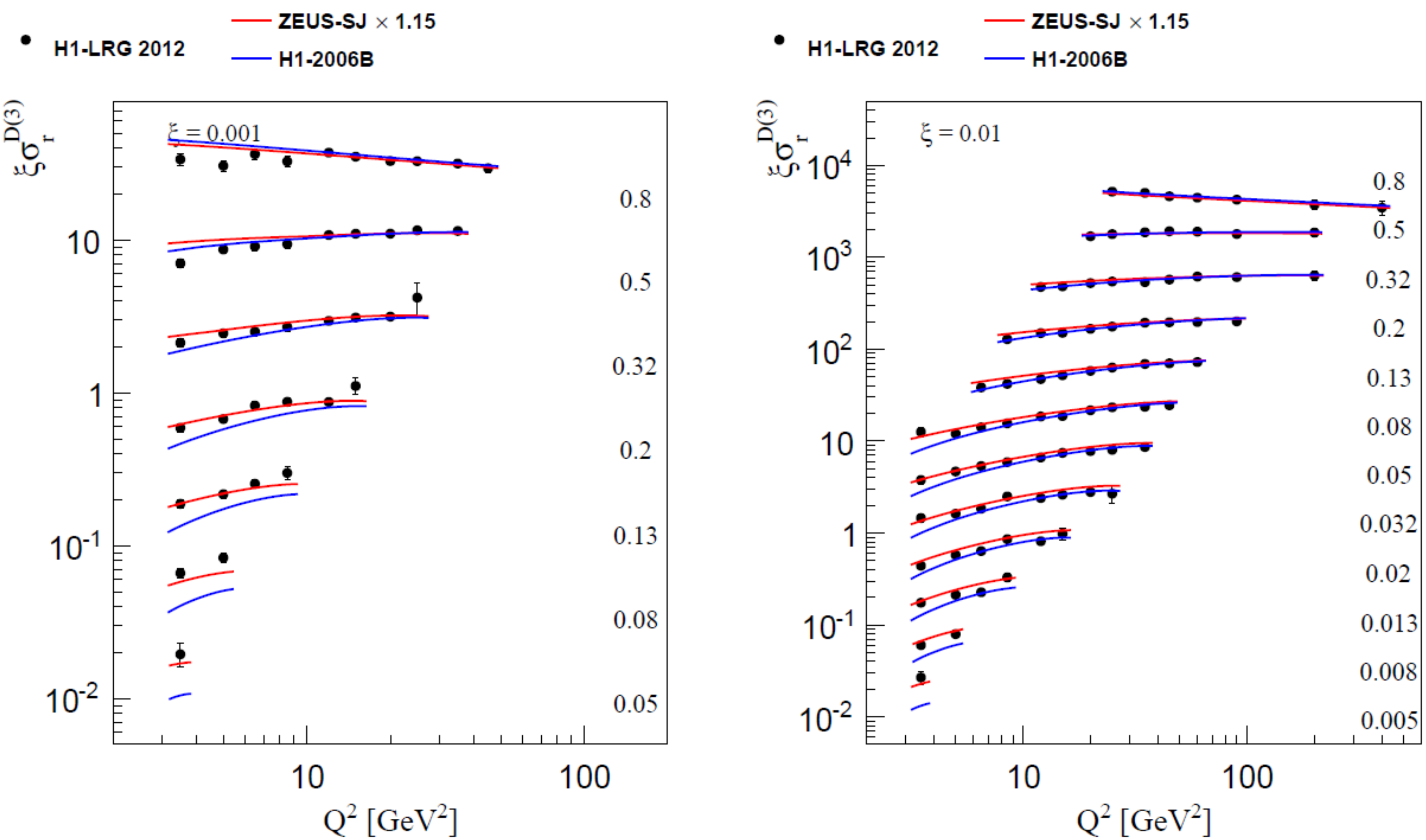

Comparison of H1-2006B and ZEUS-SJ fits to the H1-LRG 2012 data
ZEUS-SJ fit seems to better describe the data in the low β region

Phase space: HERA to LHeC to FCC-eh

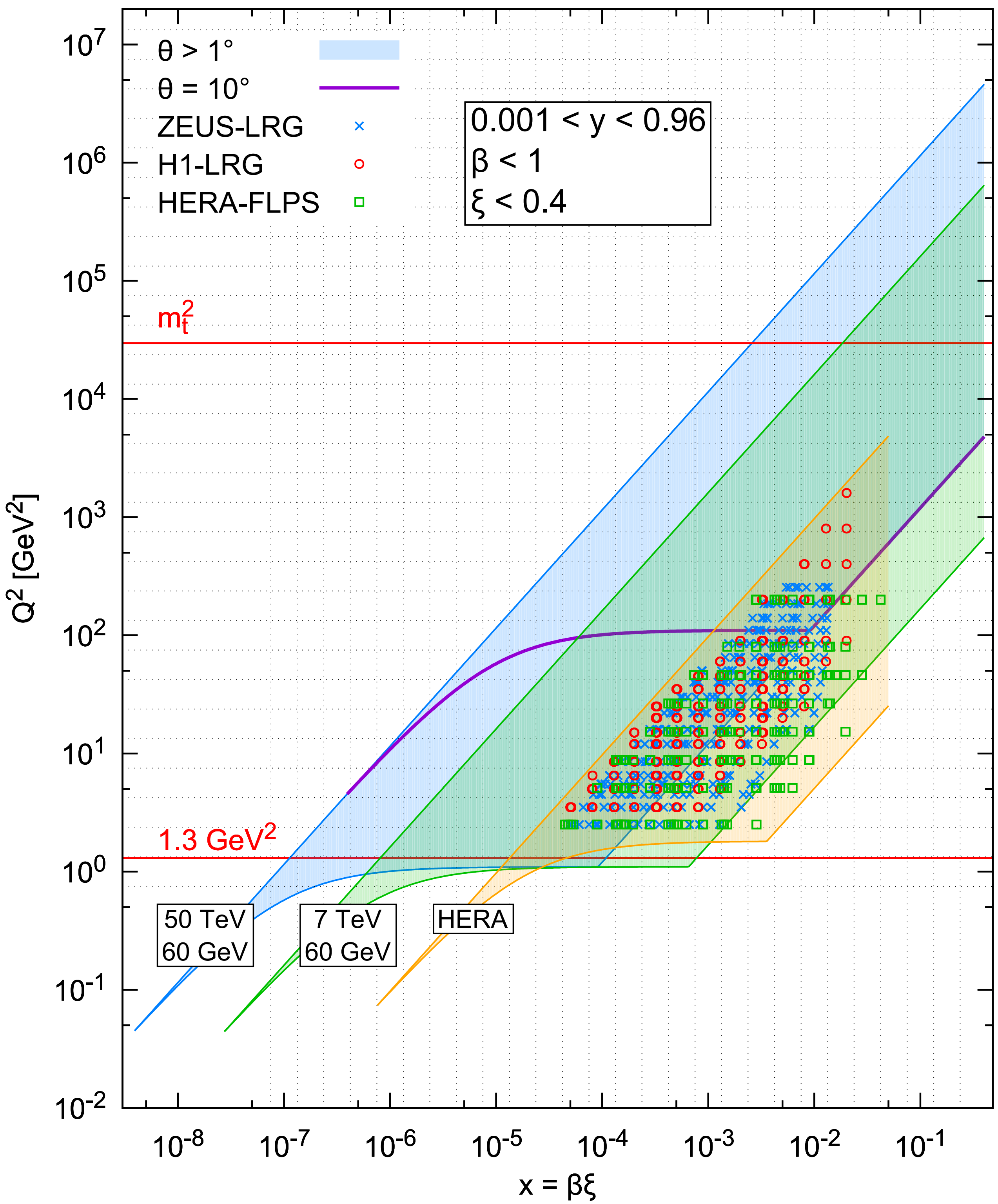

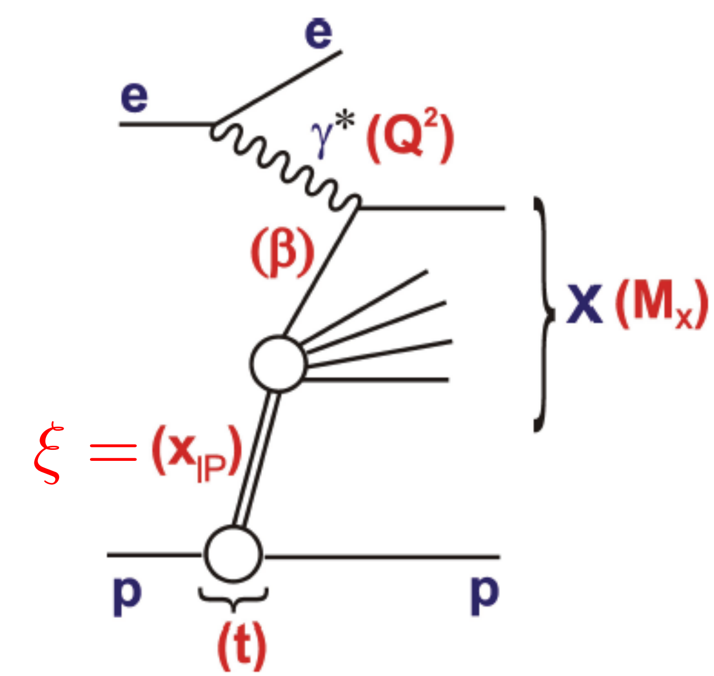

$E_e = 60\ GeV$

- $E_p = 7$ TeV vs. HERA
  - $x_{\min}$ down by factor ~20
  - $Q^2_{\max}$ up by factor ~100
- $E_p = 50$ TeV vs. 7 TeV
  - $x_{\min}$ down by factor ~10
  - $Q^2_{\max}$ up by factor ~10

LHeC phase space: (β,Q²) fixed ξ

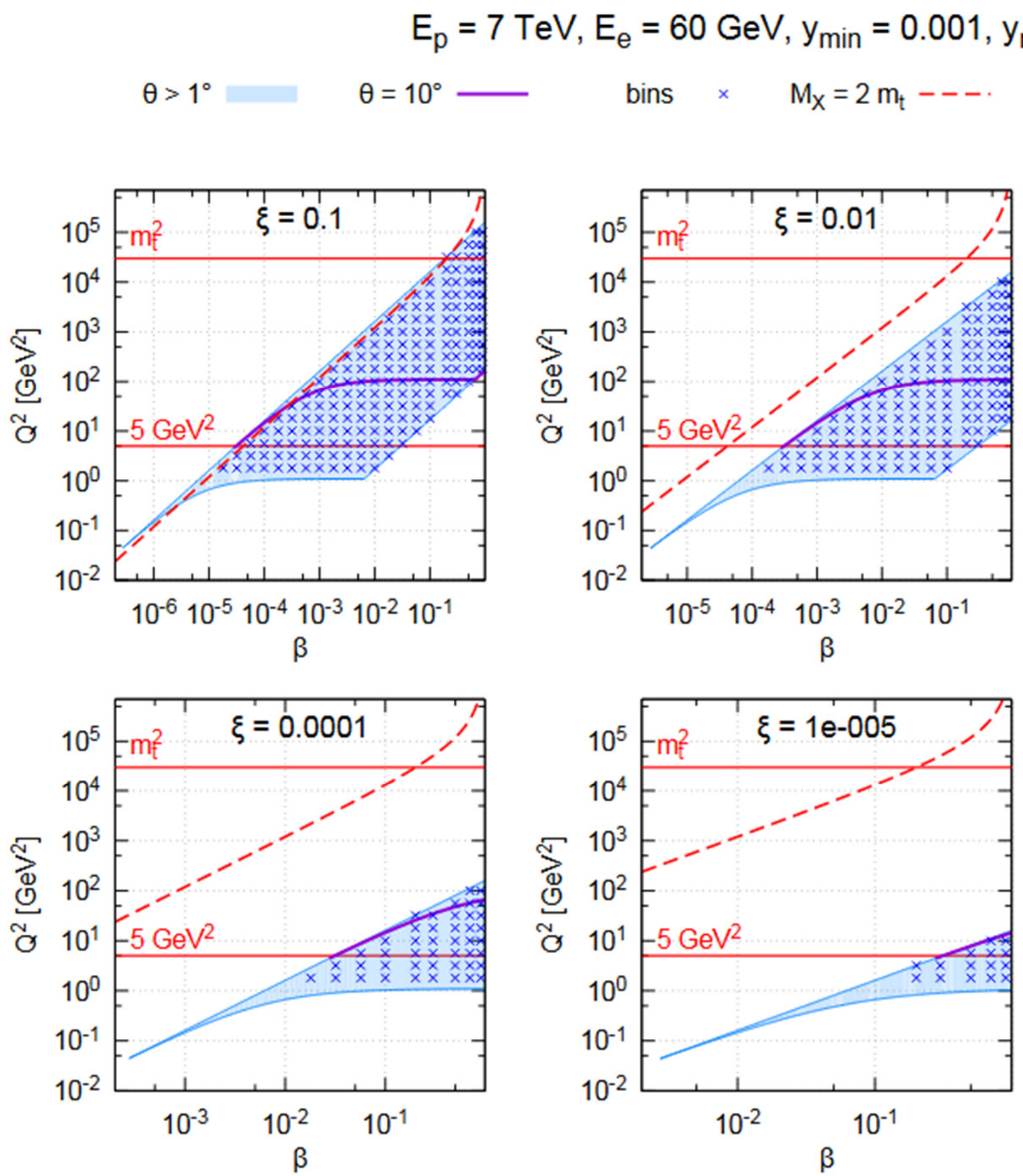

 # bins for $\xi < 0.15$

- no top
  - 1589 for $Q^2 > 1.3\ \mathrm{GeV}^2$
  - 1229 for $Q^2 > 5\ \mathrm{GeV}^2$
- with top quark
  - 17 bins more

FCC-eh phase space: (β,Q²) fixed ξ

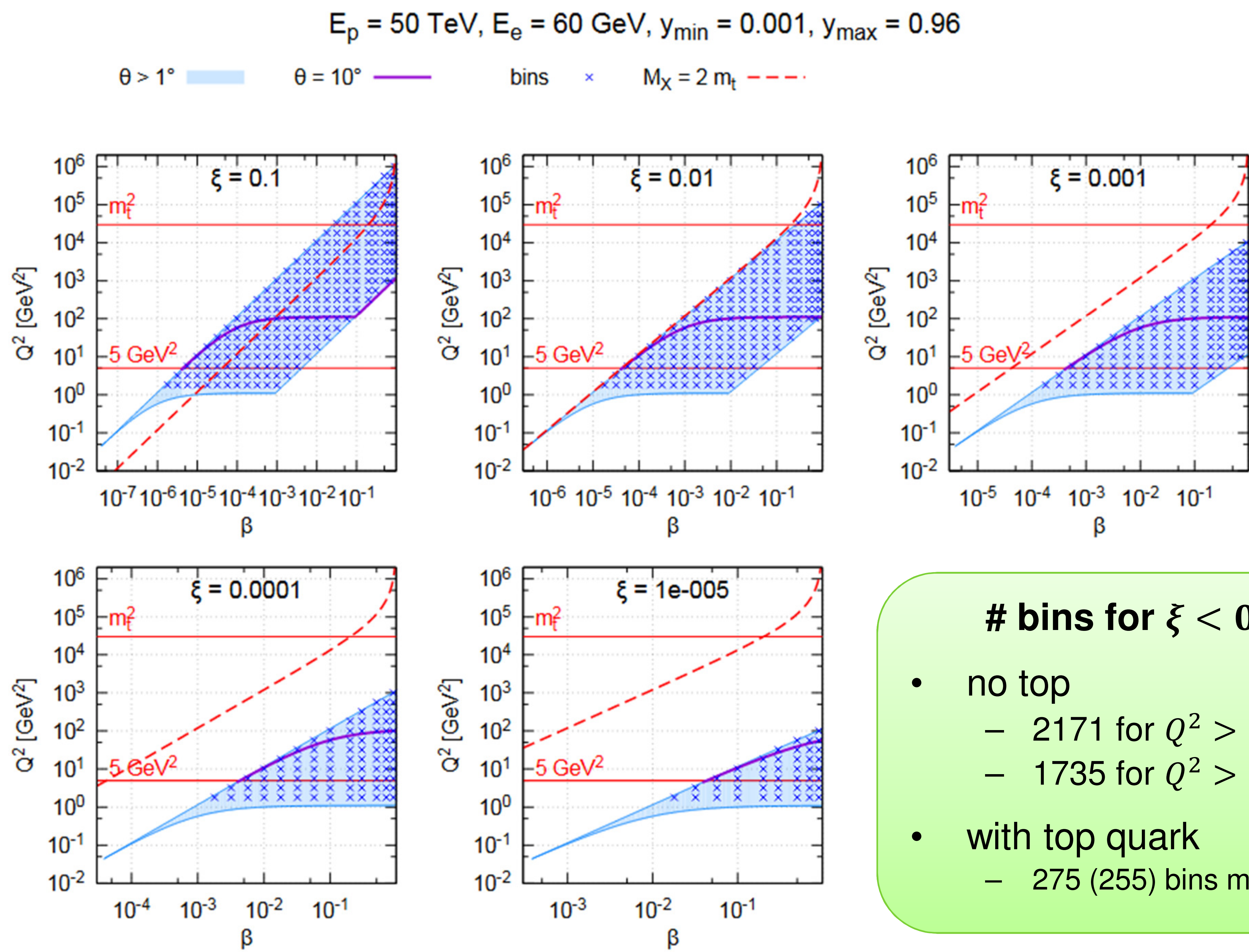

 # bins for $\xi < 0.15$

- no top
  - 2171 for $Q^2 > 1.3\ \mathrm{GeV}^2$
  - 1735 for $Q^2 > 5\ \mathrm{GeV}^2$
- with top quark
  - 275 (255) bins more

Data simulations

- Simulations based on extrapolation from ZEUS-SJ DPDFs
- VFNS scheme but no top at HERA so top contribution neglected in the simulation
- Errors simulated with 5% Gaussian noise
- Reggeon contribution is included but hard to constrain at HERA, could lead to large uncertainty in the extrapolation at ξ>0.01
- Binning to assume negligible statistical errors

Example of data: large ξ, LHeC

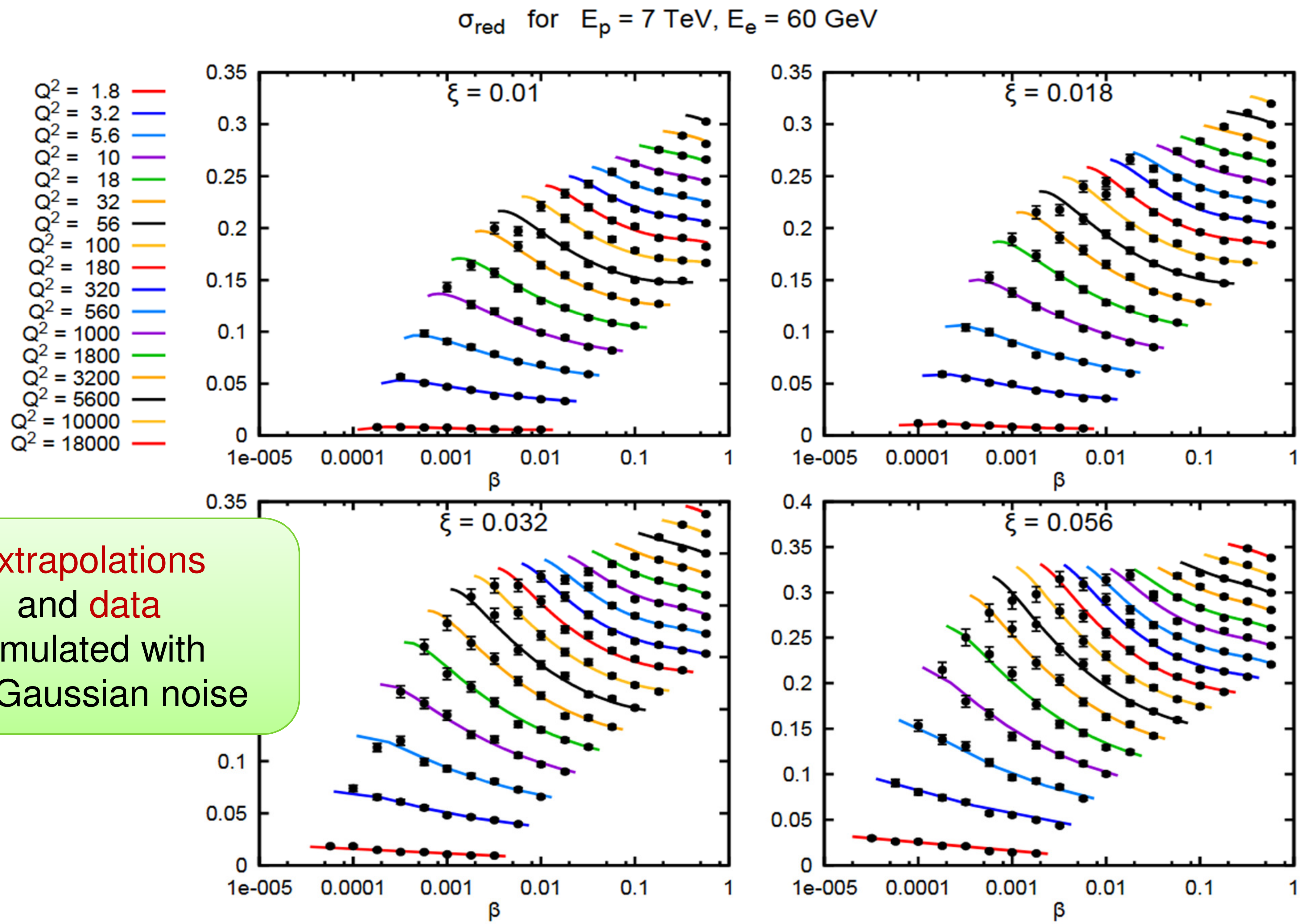

Extrapolations and data simulated with 5% Gaussian noise

Example of data: large ξ, FCC-eh

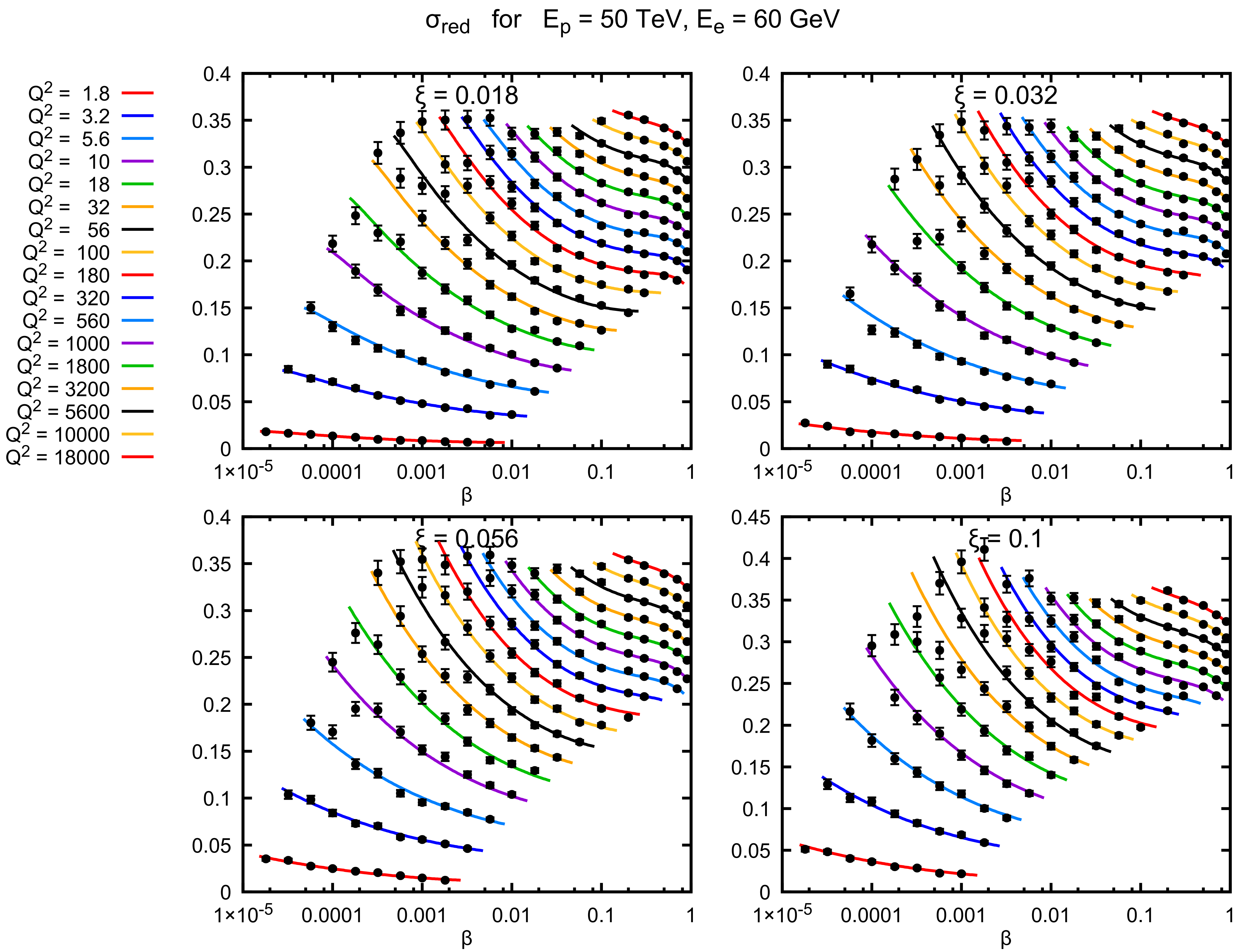

DPDFs from simulations

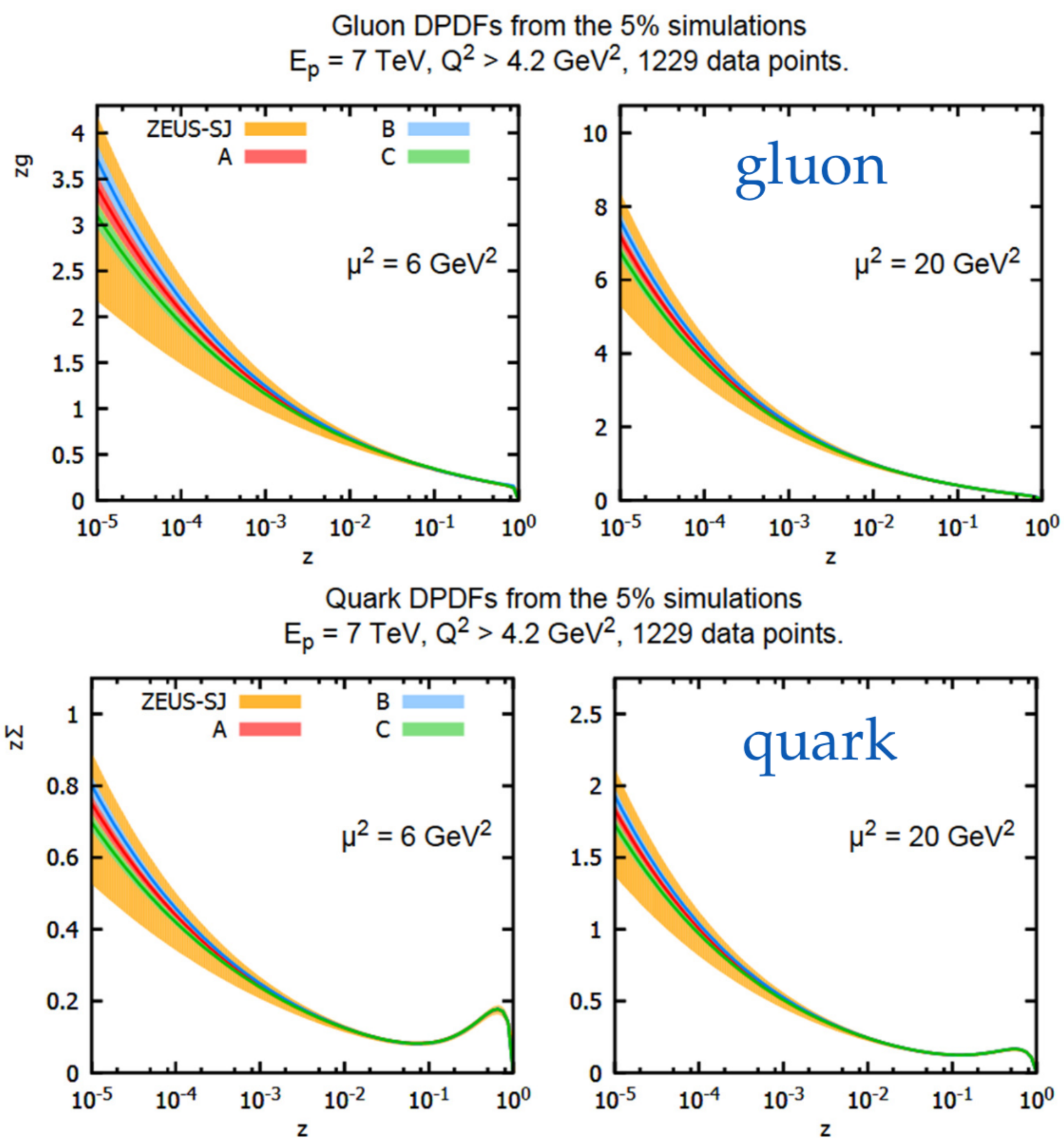

$Q^2_{\min} \approx 5\ \mathrm{GeV}^2$

$E_p = 7\ \mathrm{TeV}$

- Substantially improved accuracy wrt. HERA
- Statistical spread ~ 2 × error-band
- Statistical spreads well below error-bands for $Q^2_{\min} \approx 1.3\ \mathrm{GeV}^2$ or

DPDFs error bands

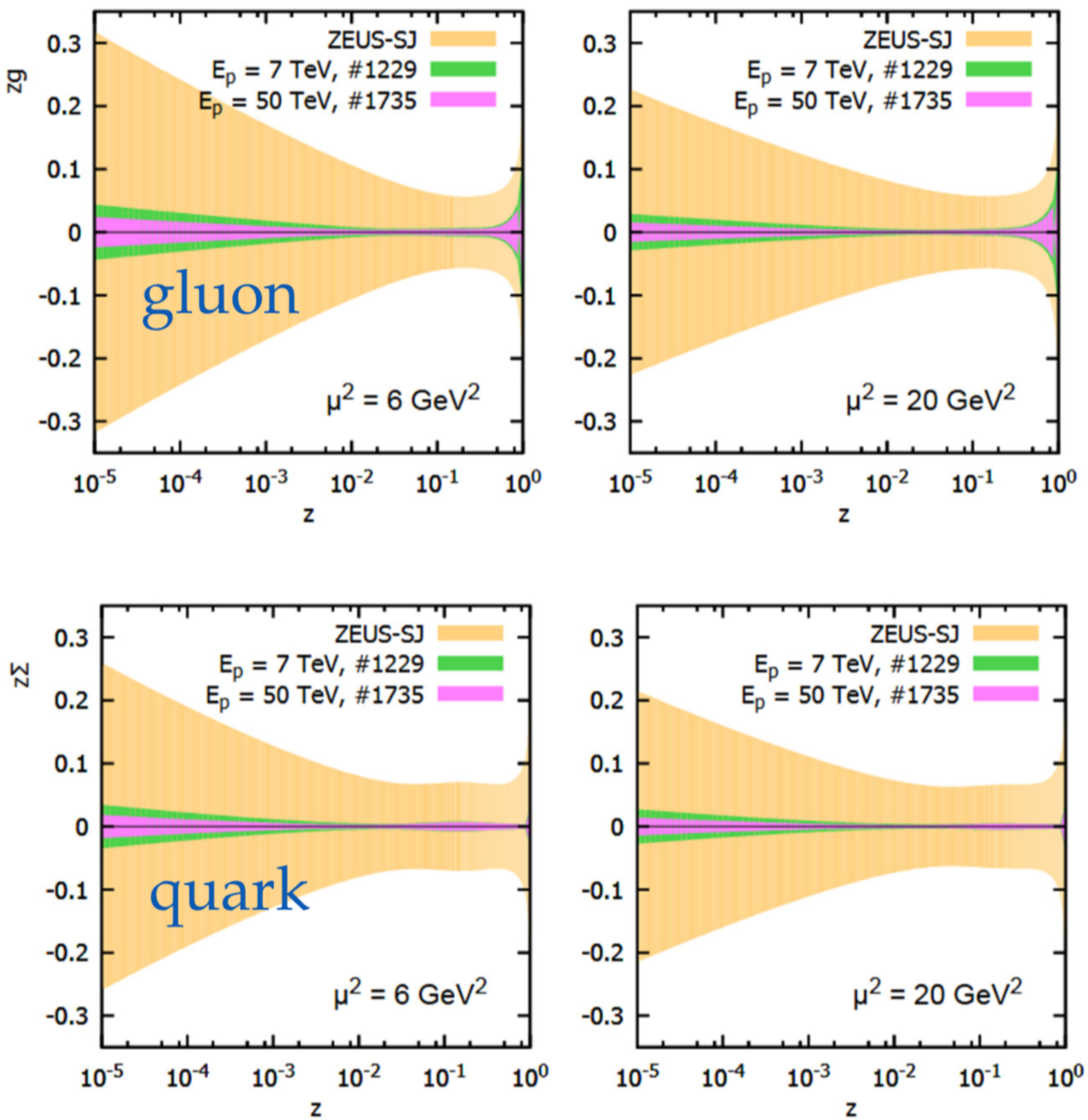

$Q^2_{\min} \approx 5\ \mathrm{GeV}^2$

Accuracy increased by

- ✓ factor ~10 for LHeC
- ✓ factor ~20 for FCC-he

Luminosity study

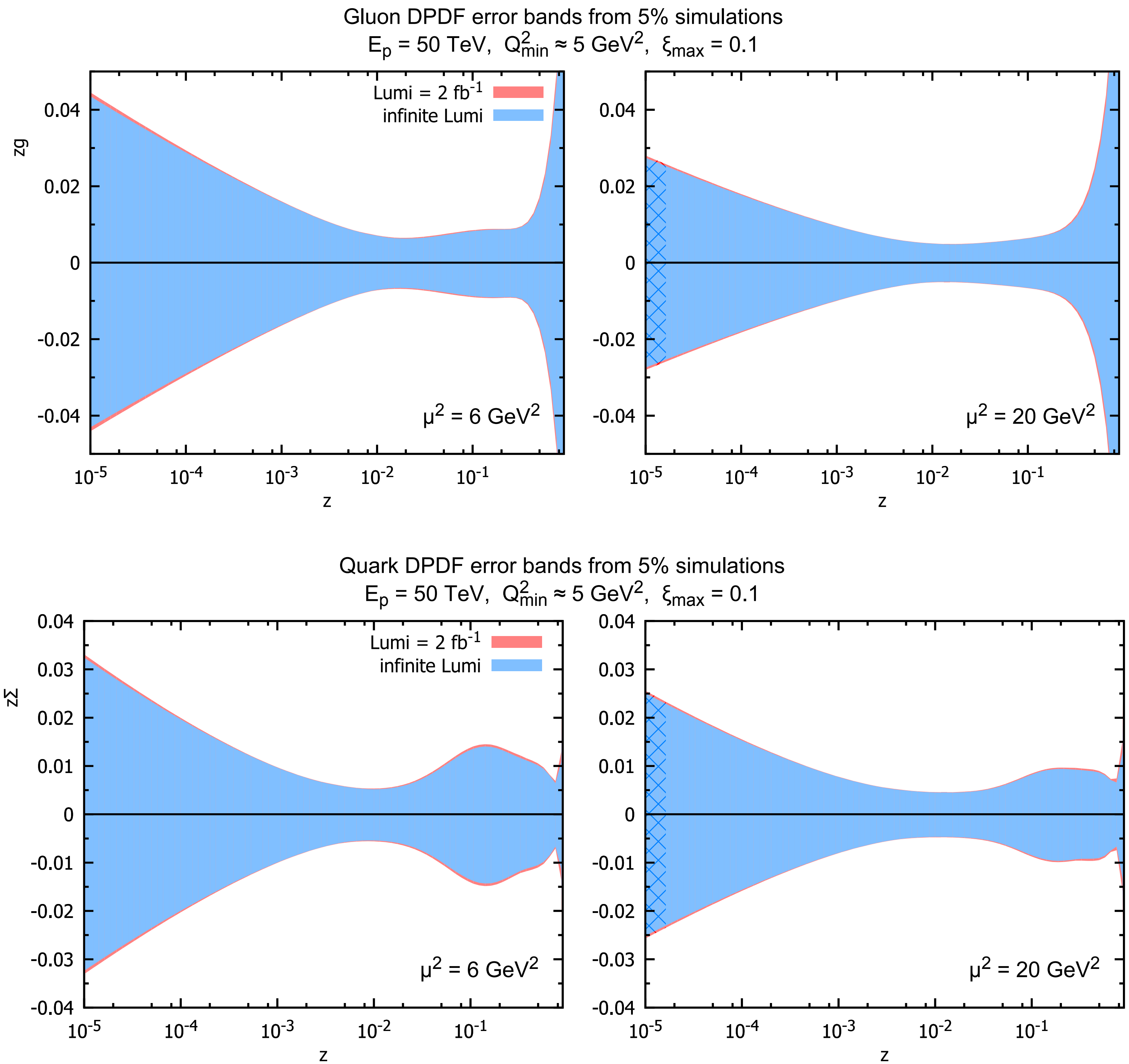

$$E_e = 60 \text{ GeV}$$
$$E_p = 50 \text{ TeV}$$
$$Q^2_{\text{min}} \simeq 5 \text{ GeV}^2$$

Comparison of 'infinite' Lumi simulation and Lumi=2 fb^{-1}

For this measurement there is negligible difference

Dependence on Q_{min}^2 and E_p

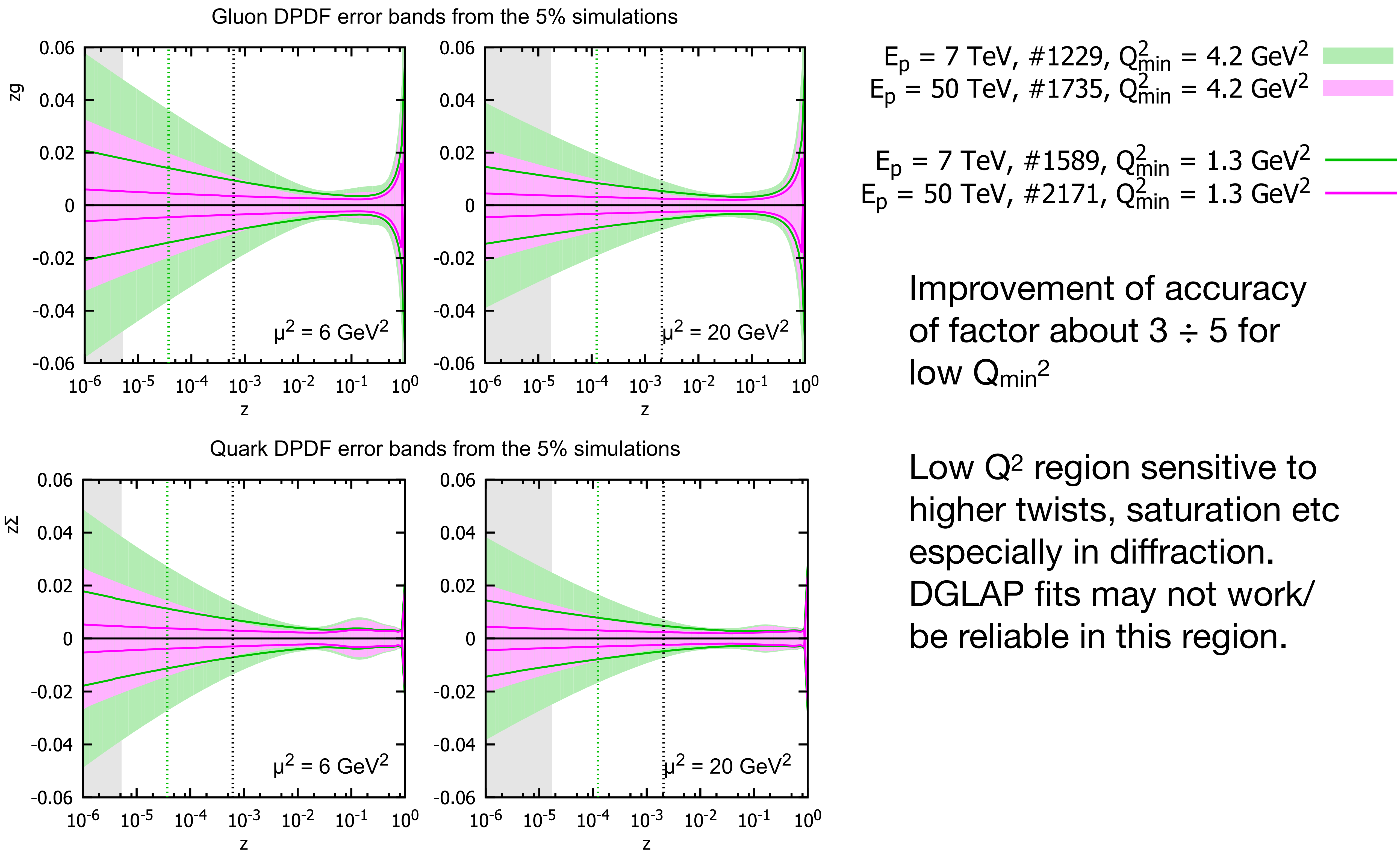

Improvement of accuracy of factor about 3 ÷ 5 for low Q_{min}^2

Low Q^2 region sensitive to higher twists, saturation etc especially in diffraction. DGLAP fits may not work/ be reliable in this region.

DPDF accuracy: top contribution

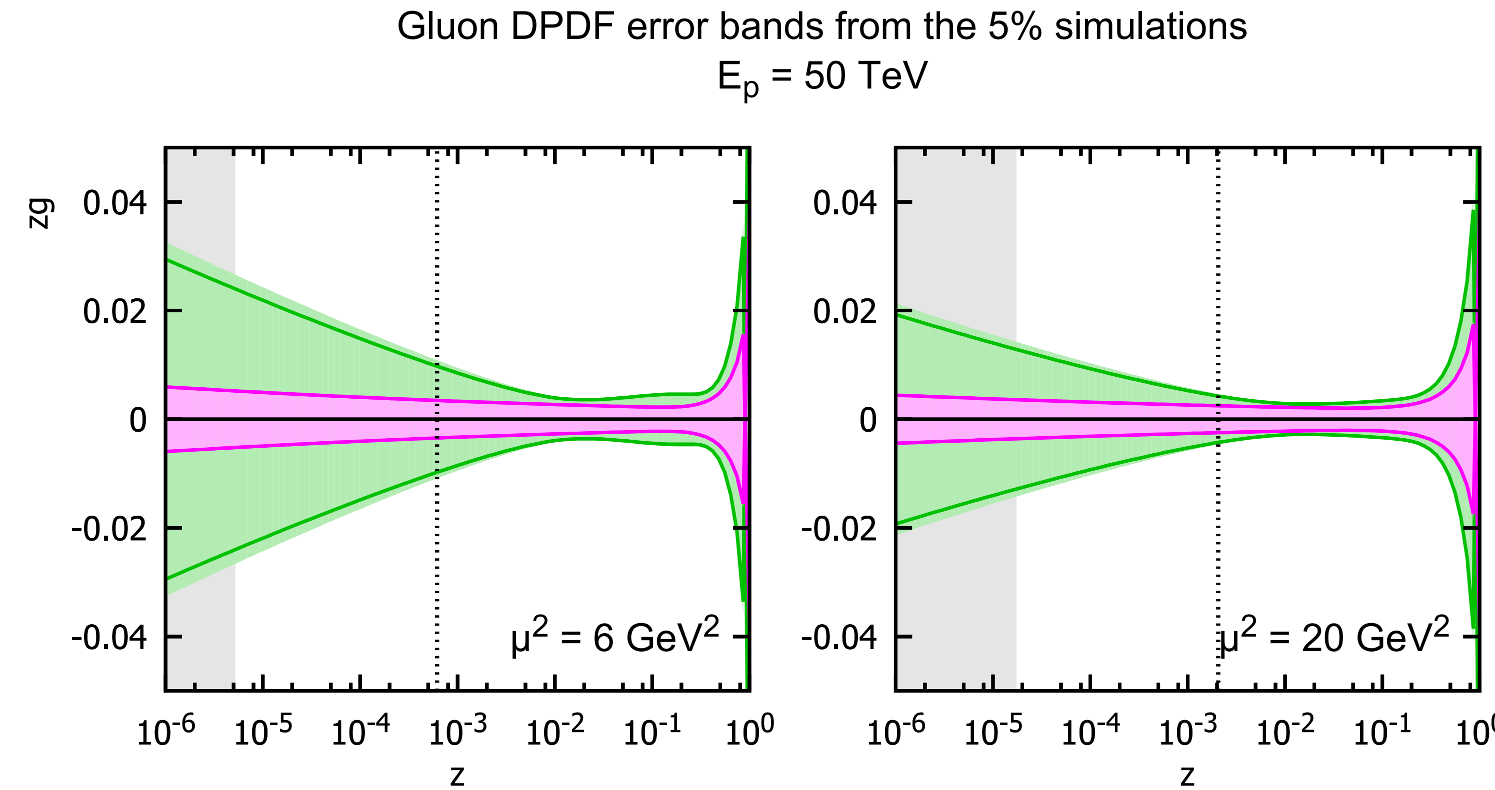

#1735, no top, Q^2_{min} = 4.2 GeV^2
#1990, w. top, Q^2_{min} = 4.2 GeV^2

#2171, no top, Q^2_{min} = 1.3 GeV^2
#2446, w. top, Q^2_{min} = 1.3 GeV^2

Top quark phase space region does not have big effect on the DPDF extraction

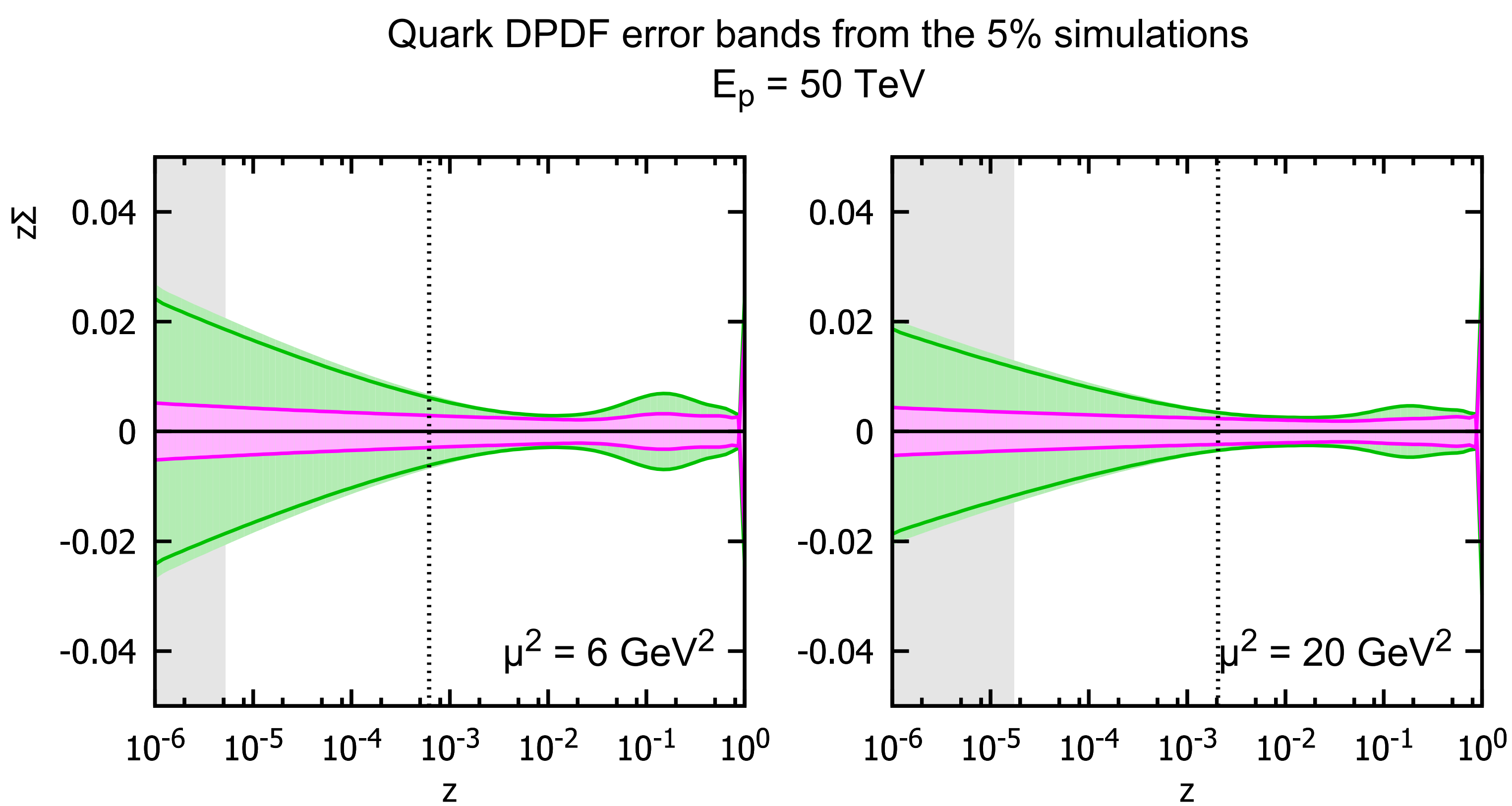

Nuclear diffractive structure functions

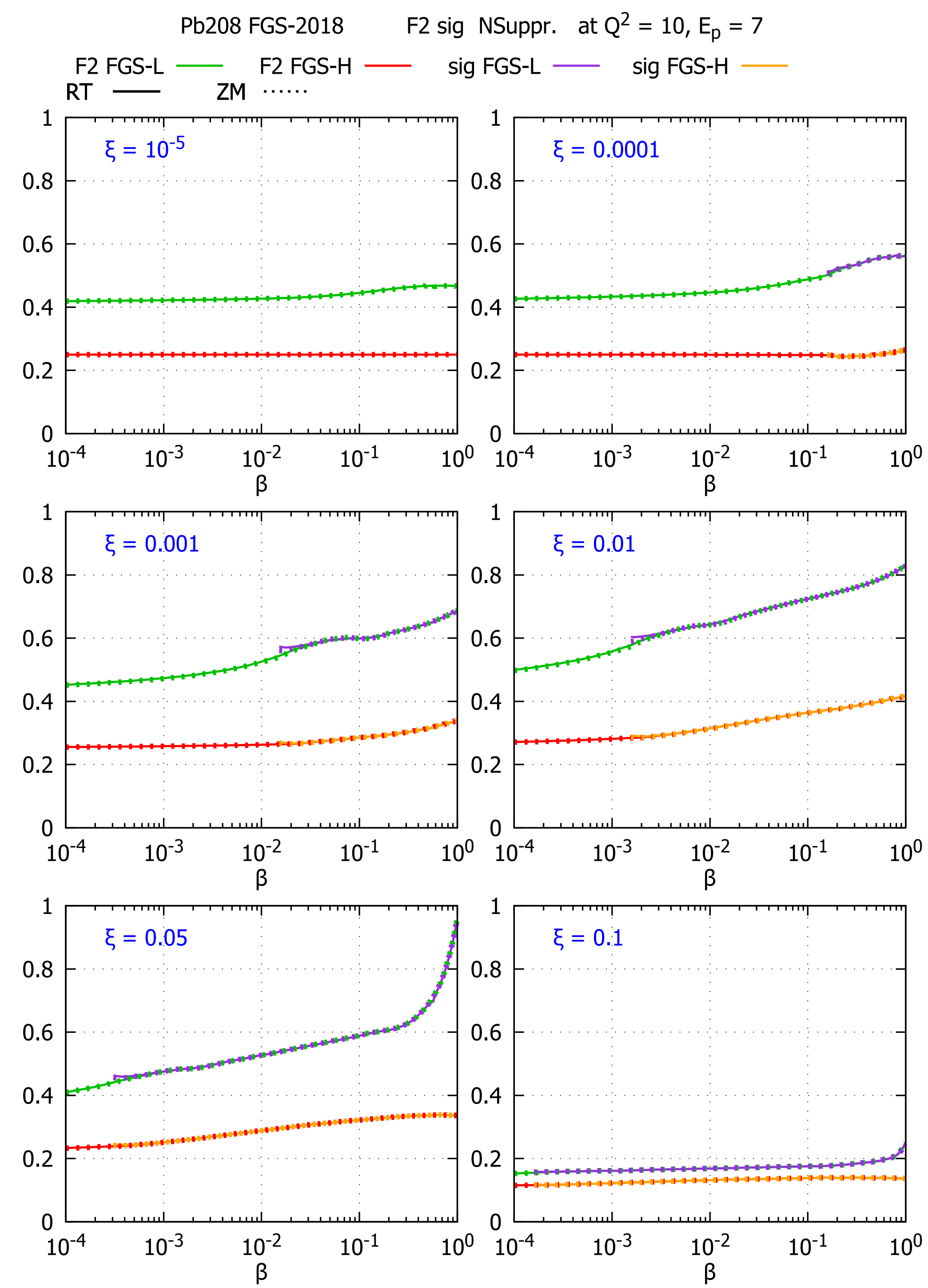

- Model for nuclear shadowing: Frankfurt,Guzey,Strikman
- Two models: high and low shadowing
- Results for nuclear ratio:

$$R_k(\beta,\xi,Q^2) = \frac{f_{k/A}^{D(3)}(\beta,\xi,Q^2)}{A\, f_{k/p}^{D(3)}(\beta,\xi,Q^2)}$$

Nuclear diffractive cross sections

LHeC

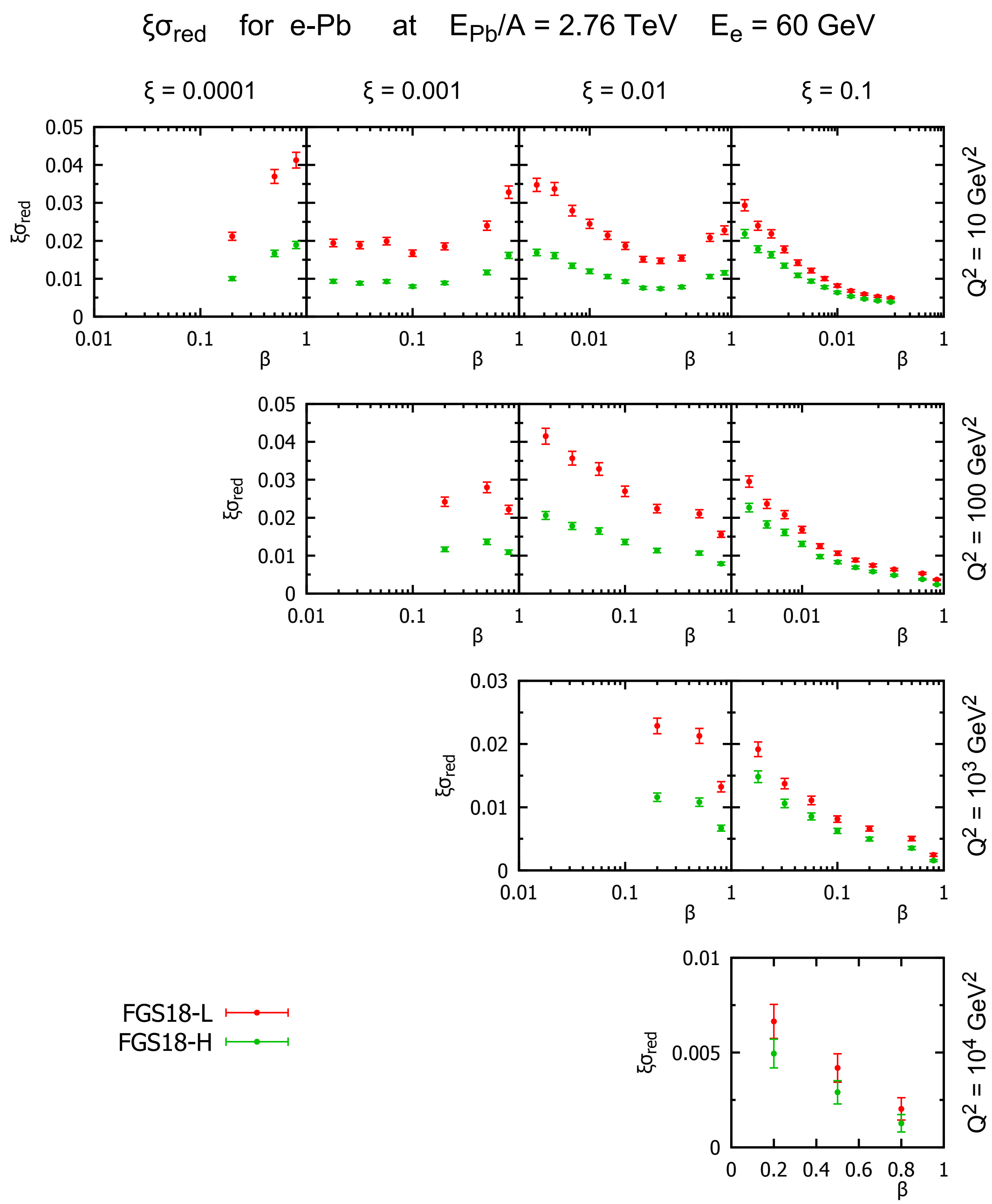

FCC-eh

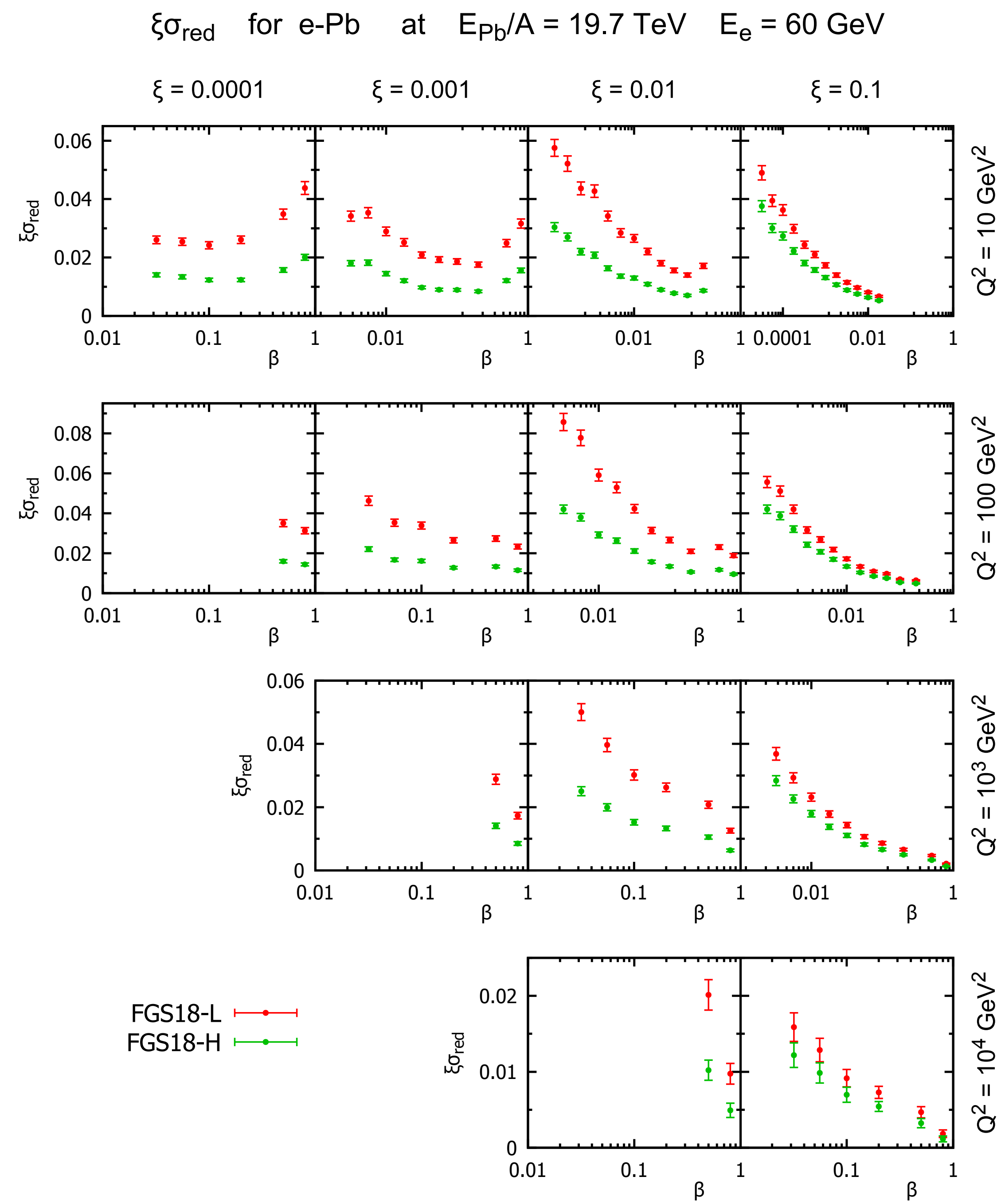

Summary and Outlook

- New possibilities for studies of diffraction at LHeC and FCC-eh.
- DPDF accuracy increased by about factor 10 at LHeC and 20 at FCC-eh.
- It is possible to constrain gluon by inclusive data alone. Diffractive dijet production was necessary at HERA to constrain the gluon, such constraints could also be included at LHeC/FCC-eh further reducing accuracy.
- Possibility of producing diffractive top. DPDF determination does not seem to be affected much by the top though.
- Lowering initial Q^2 increases the accuracy. This is the region that is expected to be very sensitive to higher twists in diffraction. Further analysis with better modeling of this region is necessary to estimate the impact of such correction.
- First analysis for diffraction in e-Pb at LHeC/FCC-eh.